Effect on Structural and Optical Properties of NiO Thin Film on Ag Incorporation

Laishram Thoibileima Chanu, Shagolsem Romeo Meitei, and Naorem Khelchand Singh

1 Introduction

In the past decades, nickel oxide (NiO)-based thin film (TF) has been employed due to the efficiency of the materials utilization and extensive improvement in suitability for a wide range of applications. NiO (p-type) is a transition metal oxide with a wide bandgap of 3.2–3.8 eV [1] and has promising properties like highly stable chemically and thermally [2, 3], and tunable optical properties [4]. NiO has been extensively studied for various applications such as photonic [5], photocatalytic [1], battery [6], sensor [7], etc. To extend the range of applicability of NiO over wide fields, tuning the properties of NiO by incorporating it with other metal oxide or metal may be effective [7–10]. Moreover, there have been reports investigating the enhanced properties by doping or incorporating with metals like lanthanum [7], lithium [6], gold [11], platinum [12], etc. Among them, silver (Ag) is the cheapest with excellent properties like good thermal and electrical conductivity, highly reflective, etc. Moreover, it is a non-reactive material, which makes it favorable to incorporate [13, 14].

In this work, we fabricate bare NiO TF and Ag incorporation NiO (Ag-NiO) TF using electron-beam (e-beam) evaporation. Comparing the deposited films, an in-depth analysis of the enhancement effect of Ag incorporation is studied with different characterizations. For structural and morphology, X-ray diffraction (XRD), as well as field-emission scanning electron microscope (FESEM) analysis, to investigate the elemental composition, energy-dispersive spectroscopy (EDS) measurement, for

L. T. Chanu (✉) · S. R. Meitei · N. K. Singh
Department of Electronics and Communication Engineering, National Institute of Technology, Chumukedima, Nagaland 797103, India
e-mail: thoibileimalaish@gmail.com

L. T. Chanu
Department of Computer Science, Tetso College Nagaland, Dimapur 797103, India

S. R. Meitei
Department of Physics, IIT (ISM Dhanbad), Dhanbad 826004, India

B. P. Swain (ed.), *Recent Advances in Materials*, Springer Proceedings in Materials 25,
https://doi.org/10.1007/978-981-99-3844-5_8

optical properties photoluminescence (PL) analysis, and absorption analysis was performed. Each characterization study was performed based on as-deposited bare NiO TF and as-deposited Ag-NiO TF.

2 Experimental Details

An e-beam evaporation technique (model—BC 300, HHV India) was employed to deposit NiO TF and Ag-NiO TF onto silicon (Si) substrate (p-type single crystal <100>) each of which cut in a dimension of 1 × 1 cm. Before the deposition, the sequential steps of cleaning the substrate were carried out using a solution of acetone, methanol, and deionized water (purity of 99.99% each) in the ultrasonic cleaner consecutively for 3 min each. After cleaning, the cleaned substrates were loaded inside the vacuum coating chamber using a substrate holder. The target source material (maintained purity 99.99%) for evaporation, NiO granules for NiO TF deposition, and Ag-NiO composite (ratio of $1_{Ag:}\ 4_{NiO}$) granules for Ag-NiO TF were utilized. Between the target source and the substrate holder, a distance of 22 cm was maintained perpendicularly. The films (bare NiO TF and Ag-NiO TF) were deposited with a consistent deposition rate of 1 Å/s and a base pressure at ~5 × 10^{-6} mbar. The depositing density of the films was monitored using digitized quartz crystal during the deposition. An in-depth study on the properties of the films has been performed with different characterizations, i.e., Rigaku Ultima IV emitting Cu Kα radiation of monochromatic X-ray (XRD) to examine the crystallinity behavior, FESEM to deduce morphology, EDS to analyze and elemental composition using ZEISS-SIGMA, 5 kV. For the optical properties analysis, PL (Hitachi F-7000 spectrophotometer), and UV-Vis spectrophotometer (Hitachi-UH-4150) were employed. All the characterization studies were performed using two samples, i.e., as-deposited bare NiO TF and as-deposited Ag-NiO TF.

3 Results and Discussion

3.1 Structure and Morphology Analysis

Figure 1 shows the XRD pattern of the bare NiO TF and Ag-NiO TF deposited on Si substrate, obtaining pure crystallographic properties. Three peaks for bare NiO TF orientations at (222), (400), and (440) phases and three peaks at (222), (400), and (440) with two peaks for Ag at (111) and (200) were observed. Both the XRD pattern shows a polycrystalline nature, and with Ag incorporation, the XRD pattern does not find any reaction phases. Moreover, (100) plane observed on both the patterns corresponds to the Si substrate [15]. For each diffraction peaks, the respective FWHM

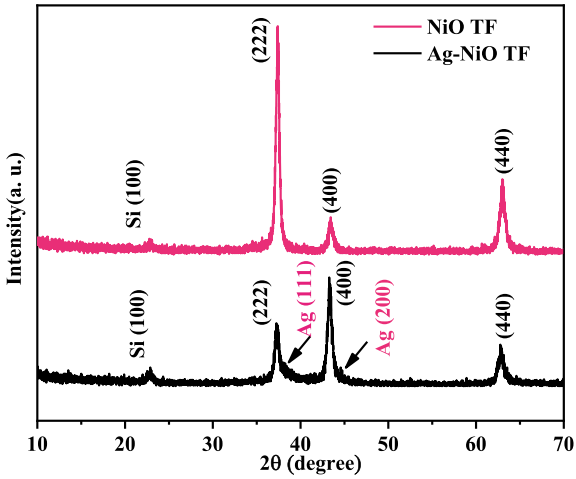

Fig. 1 Bare NiO TF and Ag-NiO TF XRD pattern

values were applied to calculate the average crystalline size 'D' implementing the Debye–Scherrer [16].

$$D = \frac{0.9 \cdot \lambda}{\beta \cdot \mathrm{Cos}\theta}, \tag{1}$$

where the X-ray radiated wavelength (1.54056 Å) denoted by 'λ', corresponding FWHM of the obtained peaks is denoted by 'β,' and Bragg's angle by 'θ.' From the evaluation of Debye–Scherrer formula, the average crystallite size was found to be 14.44 nm for bare NiO TF and 13.44 nm for Ag-NiO TF. Here, crystallite size reduction for Ag-NiO TF is observed, which may be due to integration of Ag atoms in grain boundaries as well as surface of the film. Using the Stock's Wilson relation [17], the lattice strain for both the sample was evaluated. The lattice strain seems increased from 0.00125 for NiO TF to 0.00134 for Ag-NiO TF.

Figure 2 shows the morphology of both the deposited samples using FESEM analysis. Figure 2a, b display the top-view and cross-sectional view for bare NiO TF and Ag-NiO TF, respectively. From the images, we observe the well-growth of both samples with densely packed. The acquired thickness of both samples was found to be ~375 nm. Moreover, with the Ag incorporation, the surfaces increase lattice strain as a rough appearance of the surfaces can also be seen in Fig. 2b. This result also correlates with the reduction in crystallite size in XRD analysis, which in turn arouse a surface tension and increase of stress with incorporation of Ag [18].

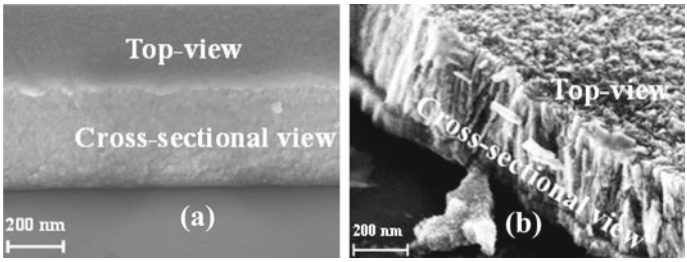

Fig. 2 Top and cross-sectional view FESEM image of **a** bare NiO TF and **b** Ag-NiO TF

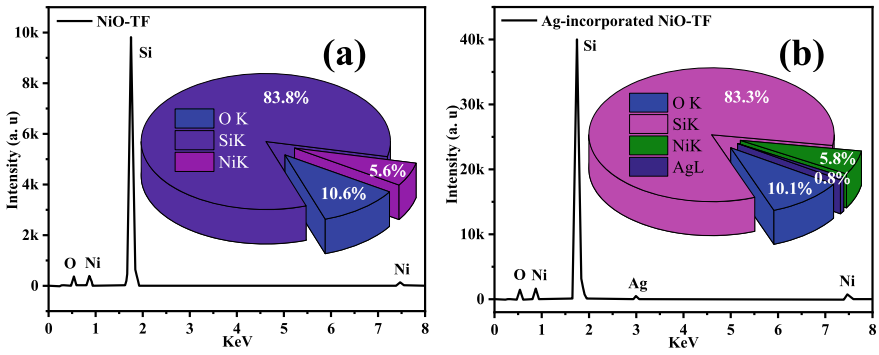

Fig. 3 EDS spectrum and atomic % analysis for **a** bare NiO TF **b** Ag-NiO TF

3.2 EDS Analysis

The elemental composition investigation using EDS analysis is shown in Fig. 3a, b. Figure 3a displays the composition of Si, Ni, and O of bare NiO TF, whereas Fig. 3b indicates the existence of Si, Ni, O, and Ag. Both the deposited films show that there are no free unwanted impurities present in them. Moreover, in Fig. 3b, the appearance of Ag supports the XRD analysis revealing separate peaks for Ag.

3.3 Optical Properties

The PL spectra of bare NiO TF and Ag-NiO TF excited at 250 nm are shown in Fig. 4. Both spectra show a wide range of UV–Vis spectral emission from 320 to 600 nm. Both films show emissions at around ~330 nm (3.75 eV), ~400 nm (3.1 eV), ~436 nm (2.84 eV), and ~467 nm (2.65 eV). The strong UV peaks at 3.75 eV and 3.1 eV can be accredited to the electronic transition of Ni^{2+} ions between the conduction band (CB) and valence band (VB) and 3.1 eV as near band edge emission [19, 20]. Further, blue emissions at 436 nm and 467 nm may be due to the trapped-electron transitions of

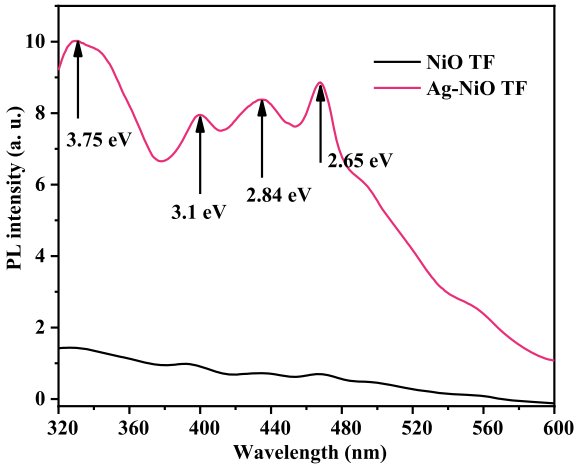

Fig. 4 PL spectra for bare NiO TF and Ag-NiO TF

nickel vacancies [21]. Comparing the emissions intensity of bare NiO and Ag-NiO TF, we can observe an increase in intensity, which may be due to the incorporated Ag behaving as a charge recombination center and the low intensity of the bare NiO reveals small amount of photogenerated carriers [8]. Related research was also reported by Romeo et al. on β-Ga_2O_3 nanowires by integrating Ag, Prasenjit et al. reported the study of Ag incorporation on TiO2 nanowires/reduced graphene oxide, employing e-beam evaporation [18, 22].

UV–Vis absorption spectra for bare NiO and Ag-NiO TF are displayed in Fig. 5a. Both spectra show the absorption edge in the UV-region and visible-region wide absorption. Comparing both spectra, the absorption intensity increased for Ag-NiO film, which indicates the improvement in absorption due to photon absorption by incorporating Ag. This can also be attributed to the numerous scatterings of light inside the nanostructure due to plasmonic effect of Ag incorporation. Figure 5b shows the bandgap calculation by plotting Tauc relation [8]. From the plot, the evaluated bandgap is found to be 3.54 eV for bare NiO TF and 3.12 eV for Ag-NiO TF. The bandgap of the films seems to decrease for Ag-incorporated films, which may be due to the shifting of free electrons between the CB and VB [18]. With the introduction of Ag, more excitation of electron occurs, that ascribe to the surface plasmon resonance of Ag. A similar study was reported by Romeo et al. for β-Ga_2O_3, Henam et al., and Suresh *et* for NiO [8, 18, 23]. However, Khedkar et al. obtained the similar results reporting that the lowering of bandgap is due to electronic interaction of Ag and NiO at the interface.

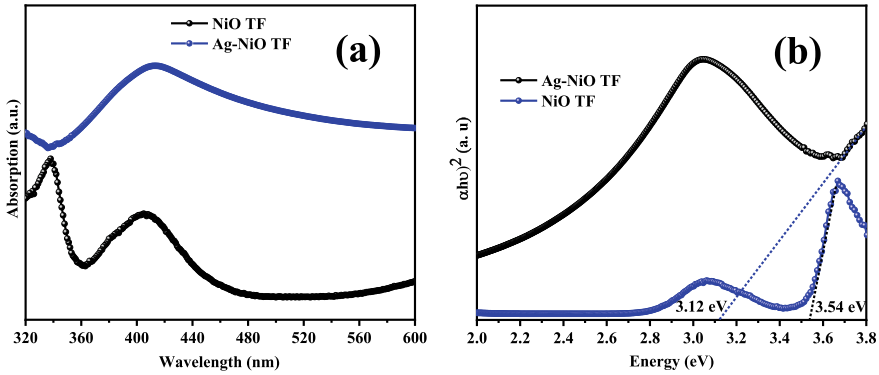

Fig. 5 **a** UV–Vis absorption spectra **b** Tauc plot of bare NiO and Ag-NiO TF

4 Conclusion

NiO TF and Ag-NiO TF have been successfully fabricated employing the e-beam evaporation method. The XRD study promotes the crystallinity of the fabricated films with an evaluated average crystallite size of 14.44 nm for bare NiO TF and 13.44 nm for Ag-NiO TF. The elemental composition for Ag incorporation is confirmed with energy-dispersive X-ray spectroscopy (EDS) study as well as XRD analysis. The benefit of Ag incorporation can be observed by PL and absorption analysis displaying enhanced intensity and improvement in absorption due to the collaborative action of Ag. The obtained results demonstrated the positive impact of Ag incorporation which can be a good candidate for various applications such as a photodetector, gas sensor, photocatalytic.

Acknowledgements We authors would like to show gratitude to the CoE in Advanced Material, and NIT Durgapur for FESEM analysis, NIT Manipur for PL analysis. We also thankful to Science & Humanities department and Electronics and Communication department, NIT Nagaland for providing XRD measurement, and for providing financial support.

References

1. Al-Ghamdi AA, Abdel-wahab MS, Farghali AA, Hasan PMZ (2016) Structural, optical and photo-catalytic activity of nanocrystalline NiO thin films. Mater Res Bull 75:71–77. https://doi.org/10.1016/J.MATERRESBULL.2015.11.027
2. Zhang X, Zhang Y, Zhao B, Lu S, Wang H, Liu J, Yan H (2015) Improvement on optical modulation and stability of the NiO based electrochromic devices by nanocrystalline modified nanocomb hybrid structure. RSC Adv 5:101487–101493. https://doi.org/10.1039/c5ra16876g
3. Palmer DA, Bénézeth P, Xiao C, Wesolowski DJ, Anovitz LM (2011) Solubility measurements of crystalline NiO in aqueous solution as a function of temperature and pH. J Solution Chem 40:680–702. https://doi.org/10.1007/s10953-011-9670-x

4. Al-Kuhaili MF, Ahmad SHA, Durrani SMA, Faiz MM, Ul-Hamid A (2015) Application of nickel oxide thin films in NiO/Ag multilayer energy-efficient coatings. Mater Sci Semicond Process 39:84–89. https://doi.org/10.1016/j.mssp.2015.04.049
5. Saha B, Sarkar K, Bera A, Deb K, Thapa R (2017) Schottky diode behaviour with excellent photoresponse in NiO/FTO heterostructure. Appl Surf Sci 418:328–334. https://doi.org/10.1016/j.apsusc.2017.01.142
6. Liu H, Wang G, Liu J, Qiao S, Ahn H (2011) Highly ordered mesoporous NiO anode material for lithium ion batteries with an excellent electrochemical performance. J Mater Chem 21:3046–3052. https://doi.org/10.1039/c0jm03132a
7. Mrabet C, ben Amor M, Boukhachem A, Amlouk M, Manoubi T (2016) Physical properties of La-doped NiO sprayed thin films for optoelectronic and sensor applications. Ceram Int 42:5963–5978. https://doi.org/10.1016/j.ceramint.2015.12.144
8. Pandey SK, Tripathi MK, Ramanathan V, Mishra PK, Tiwary D (2021) Highly facile Ag/NiO nanocomposite synthesized by sol-gel method for mineralization of rhodamine B. J Phys Chem Solid 159. https://doi.org/10.1016/j.jpcs.2021.110287
9. Na D-M, Satyanarayana L, Choi G-P, Shin Y-J, Park JS (2005) Surface morphology and sensing property of NiO-WO 3 thin films prepared by thermal evaporation. Sensors 5:519–528. http://www.mdpi.org/sensors
10. Karimi- M, Behpour M, Babaheidari AK, Saberi Z (2017) Efficiently enhancing photocatalytic activity of NiO-ZnO doped onto nanozeoliteX by synergistic effects of p-n heterojunction, supporting and zeolite nanoparticles in photo-degradation of Eriochrome Black T and Methyl Orange. J Photochem Photobiol A Chem 346:133–143. https://doi.org/10.1016/j.jphotochem.2017.05.038
11. Mattei G, Mazzoldi P, Post ML, Buso D, Guglielmi M, Martucci A (2007) Cookie-like Au/NiO nanoparticles with optical gas-sensing properties. Adv Mater 19:561–564. https://doi.org/10.1002/adma.200600930
12. Kim SS, Park KW, Yum JH, Sung YE (2006) Pt-NiO nanophase electrodes for dye-sensitized solar cells. Sol Energy Mater Sol Cells 90:283–290. https://doi.org/10.1016/j.solmat.2005.03.015
13. Hameed MA, Ali OA, Al-Awadi SSM (2020) Optical properties of Ag-doped nickel oxide thin films prepared by pulsed-laser deposition technique. Optik (Stuttg), 206. https://doi.org/10.1016/j.ijleo.2020.164352
14. Reddy YAK, Reddy AS, Reddy PS (2014) Effect of oxygen partial pressure on the properties of NiO-Ag composite films grown by DC reactive magnetron sputtering. J Alloys Compd 583:396–403. https://doi.org/10.1016/j.jallcom.2013.08.180
15. Miyata H, Kuroda K (1999) Preferred alignment of mesochannels in a mesoporous silica film grown on a silicon (110) surface. J Am Chem Soc 121:7618–7624. https://doi.org/10.1021/ja990758m
16. El-Nahass MM, Emam-Ismail M, El-Hagary M (2015) Structural, optical and dispersion energy parameters of nickel oxide nanocrystalline thin films prepared by electron beam deposition technique. J Alloys Compd 646:937–945. https://doi.org/10.1016/j.jallcom.2015.05.217
17. Stokes AR, Wilson AJC (1944) The diffraction of X-rays by distorted crystal aggregates-I. In: Proceedings of Physical Society, 56, 174. https://doi.org/10.1088/0959-5309/56/3/303/meta
18. Meitei SR, Ngangbam C, Singh NK (2021) Microstructural and optical properties of Ag assisted β-Ga_2O_3 nanowires on silicon substrate. Opt Mater (Amst) 117. https://doi.org/10.1016/j.optmat.2021.111190
19. Chakrabarty S, Chatterjee K (2011) Synthesis and optical manifestation of NiO-silica nanocomposite. ISRN Nanotech 2011:1–6. https://doi.org/10.5402/2011/719027
20. Karthikeyan B, Pandiyarajan T, Hariharan S, Ollakkan MS (2016) Wet chemical synthesis of diameter tuned NiO microrods: microstructural, optical and optical power limiting applications. Cryst Eng Comm 18:601–607. https://doi.org/10.1039/c5ce02232k
21. Jayalakshmi G, Saravanan K, Navas J, Arun T, Panigrahi BK (2019) Fabrication of p-NiO nanoflakes/n-Si(100) heterojunction architecture for high sensitive photodetectors. J Mater Sci: Mater Electron 30:6811–6819. https://doi.org/10.1007/s10854-019-00993-y

22. Deb P, Dhar JC (2020) Boosted photoresponsivity using silver nanoparticle decorated TiO2 nanowire/reduced graphene oxide thin-film heterostructure. Nanotechnology 31. https://doi.org/10.1088/1361-6528/ab8084
23. Devi HS, Singh TD, Singh NR (2017) Green synthesis and catalytic activity of composite NiO-Ag nanoparticles for photocatalytic degradation of dyes